American Mineralogist, Volume 77, pages 146–155, 1992

Selective preservation of melt inclusions in igneous phenocrysts

Stephen Tait

Laboratoire de dynamique des systèmes géologiques, Université de Paris 7 et Institut de Physique du Globe, 4 Place Jussieu, 75252 Paris Cedex 05, France

Abstract

Phenocrysts that contain melt and gas inclusions experience dilatational stresses during eruptions because the bulk modulus of silicate melt is an order of magnitude less than the elastic moduli of crystals and because dissolved volatile components can exsolve in response to decompression. We present a physical model in which the evolution of pressure inside an inclusion is coupled with elastic deformation of the host crystal during ascent. This deformation is small, and only limited decompression of inclusions can take place, which keeps most volatile molecules in solution. For subaerial eruptions ΔP, the difference between the pressure within the inclusion and that outside the crystal is typically within 80–100% of the pressure at which the inclusion was formed. For submarine eruptions, ΔP is reduced by an amount corresponding to the weight of overlying H_2O. All else being equal, ΔP is higher for an inclusion containing a gas bubble at the time of trapping than for a pure melt inclusion. Stresses in the host fall off rapidly over a distance similar to inclusion radius, and for virtually all common inclusion sizes, the host should behave as an effectively infinite environment. Cracks in the host are likely to nucleate on preexisting microfractures that intersect the inclusion walls, and simple arguments support the notion that the stress needed to open a crack increases with decreasing length of microfracture. This suggests that the easiest microfracture to open will be of a length approximately equal to the inclusion radius and hence that smaller inclusions may withstand greater overpressures than larger inclusions. Quantitative estimates suggest that cracking of host crystals should be common, even those formed in shallow crustal magma chambers. If rapid exsolution follows cracking, decrepitation results and the inclusion contents escape. If kinetic effects substantially retard exsolution, rapid eruption and quenching of melt in the inclusion may trap volatiles before decrepitation occurs. The preservation of inclusions is likely to depend on the depth of formation, inclusion size, and the physical regime of eruption.

Introduction

In igneous and metamorphic geological environments, growth of silicate minerals often entails the isolation of inclusions of silicate melt or fluid species such as H_2O or CO_2. At the depth of formation, the external confining pressure exactly balances pressure within the inclusion and the crystal experiences no resultant stress. When the external pressure is reduced, a net stress field is produced because the equation of state of the inclusion contents differs from that of the host crystal. In spite of the extensive base of observations on inclusions in igneous and metamorphic minerals—see Roedder (1984) for a comprehensive literature summary—much less quantitative attention has been given to the stresses induced in host crystals or the behavior of the inclusion contents due to pressure changes in the environment. Gillet et al. (1984) gave an elastic model of the decompression during uplift and cooling of an inclusion of one mineral within another of differing elastic properties with application to metamorphic rocks, but not much is known about the behavior during decompression of melt and gas inclusions in elastic host crystals.

The pressure-temperature paths followed by metamorphic rocks may differ considerably according to tectonic environment. In this paper, we concentrate on the igneous environment and the ascent of magma in an eruption conduit to the Earth's surface, which represents a simpler case of decompression under approximately isothermal conditions. We calculate the elastic stresses induced in the host and couple these equations to those describing the chemical equilibrium between silicate melt and exsolved gas within the inclusion. We discuss the mechanism by which fractures may develop in host crystals and the quantitative implications for the preservation of inclusions under terrestrial eruption conditions.

On arrival at the surface, the melt inclusions are quenched to glass, and gas bubbles of various sizes are often present. Chemical compositions of inclusions are commonly used to make inferences about conditions in a magma chamber prior to an eruption. It is commonly assumed that the amounts of volatiles dissolved in glass

0003–004X/92/0102–0146$02.00

are equal to those dissolved in the silicate liquid from which the host crystals formed. Presumably the trapped melt was protected from degassing by the crystalline host during ascent in the conduit. The volatiles dissolved in magma can yield estimates of gas saturation pressures that are important for eruption triggering (Blake, 1984; Tait et al., 1989), the mass flux of an eruption, and fragmentation phenomena (Wilson and Head, 1981; Vergniolle and Jaupart, 1986). In this paper, we aim to provide the beginnings of a physical framework within which evidence from inclusion studies may be assessed. While the current article was in the review process, we became aware of a recent paper (Wanamaker et al., 1990) concerned with the decrepitation of CO_2 inclusions in San Carlos olivines, which gives an analysis with some similarities. They give a more detailed analysis of fracture propagation and healing but only brief attention to the inclusion contents.

Deformation mechanisms

One mechanism by which elastic stresses might be dissipated is that of viscous flow of the host mineral grains. In Appendix 1 we estimate the time scale of this viscous dissipation. We obtain values of 10^6 yr for minerals at the liquidus temperatures of mafic magmas, implying that viscous release of elastic stresses may be neglected on the time scale of an eruption. Metamorphic minerals, although more slowly decompressed by uplift and erosion processes, are at much lower temperatures, and hence higher viscosities apply. In short, viscous dissipation seems unlikely to be important in geological circumstances, although one might envisage some special P-T paths for metamorphic minerals undergoing uplift or the presence of other factors that can produce a large reduction of viscosity, such as exceptionally high dislocation density or proximity to a phase transition (Green and Guegen, 1983; Darot et al., 1985), and might allow sufficient time for some viscous dissipation of elastic stresses to occur. For most geological conditions, the important aspects to quantify are the elastic deformation of a crystal containing an overpressured inclusion, the behavior of the inclusion contents, and the conditions under which rupture of host crystals may be anticipated.

Elastic deformation of a crystal containing a pressurized spherical cavity

The inclusion is, for mathematical convenience, assumed to be spherical and situated at the center of a linearly elastic, spherical crystal (Fig. 1a). These assumptions constrain all displacements to be radial, and in spherical polar coordinates (r,θ,ϕ) the continuity equation for the displacement (u_r) is (e.g., Timoshenko and Goodier, 1982)

$$\frac{d}{dr}\left(\frac{du_r}{dr} + \frac{2u_r}{r}\right) = 0. \quad (1)$$

The general solution of Equation 1 is

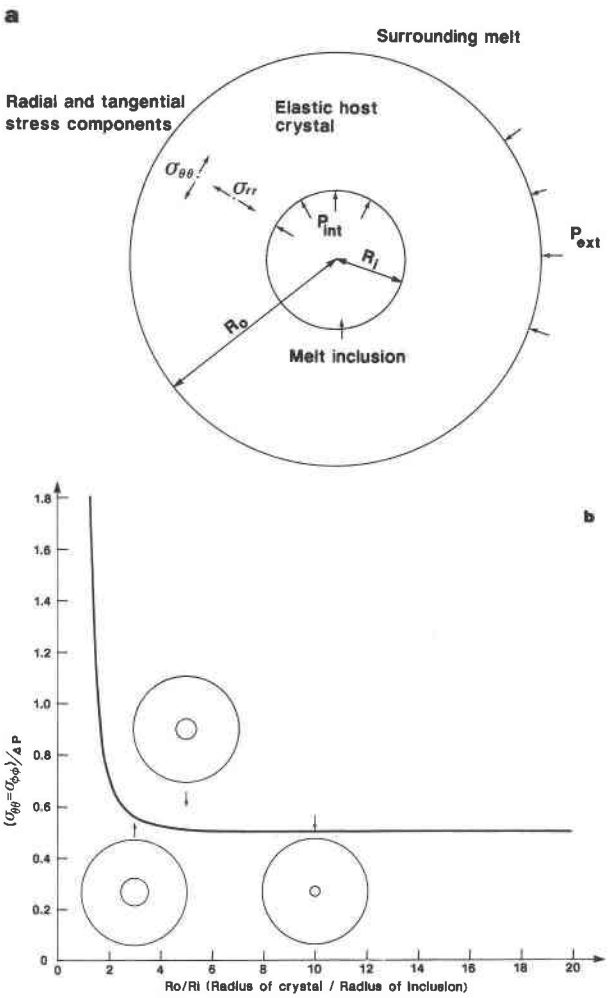

Fig. 1. (a) Sketch illustrating the geometry of the crystal and inclusion considered. (b) The tangential stresses at the inclusion wall normalized by the overpressure within the inclusion as a function of the ratio of the radius of the crystal to that of the inclusion. Because of the spherical symmetry, $\sigma_{\theta\theta} = \phi_{\phi\phi}$. The limit of $\sigma/\Delta P = 0.5$ valid for infinite R_o/R_i is rapidly attained, implying that host crystals behave as infinite environments for essentially all common inclusion sizes.

$$u_r = C_1 r + \frac{C_2}{R^2} \quad (2)$$

where C_1 and C_2 are constants. The stress components are

$$\text{radial: } \sigma_{rr} = 3C_1\beta_c - \frac{4C_2\mu_c}{r^3} \quad (3a)$$

$$\text{tangential: } \sigma_{\theta\theta} = \sigma_{\phi\phi} = 3C_1\beta_c + \frac{2C_2\mu_c}{r^3} \quad (3b)$$

where β_c and μ_c are the bulk modulus and shear modulus (rigidity) of the crystal, respectively. The boundary conditions are

$$\sigma_{rr} = -P_{\text{int}} \quad \text{at } r = R_i \tag{4a}$$
$$\sigma_{rr} = +P_{\text{ext}} \quad \text{at } r = R_o. \tag{4b}$$

P_{int}, the pressure within the inclusion, is directed outward and P_{ext}, the pressure outside the crystal is directed inward. Solving for C_1 and C_2 and substituting into Equation 2 gives the volume change (ΔV) of the inclusion:

$$\Delta V = 4\pi R_i^2 u_{r(r=R_i)} = \frac{4\pi R_i^3}{(R_o^3 - R_i^3)}\left(\frac{R_i^3}{3\beta_c} + \frac{R_o^3}{4\mu_c}\right)\cdot\Delta P \tag{5}$$

where $\Delta P = P_{\text{int}} - P_{\text{ext}}$. The fractional volume change is

$$\frac{\Delta V}{V_o} = \frac{3}{[(R_o/R_i)^3 - 1]}\left[\frac{1}{3\beta_c} + \frac{(R_o/R_i)^3}{4\mu_c}\right]\cdot\Delta P = \Gamma\cdot\Delta P \tag{6}$$

where V_o is the original volume. The tangential stresses at $r = R_i$ are

$$\sigma_{\theta\theta} = \sigma_{\phi\phi} = \frac{R_i^3}{R_o^3 - R_i^3}\left[1 + \frac{(R_o/R_i)^3}{2}\right]\cdot\Delta P. \tag{7}$$

In the limit of large R_o/R_i, Γ reduces to $3/4\mu_c$ and $\sigma_{\theta\theta} = \sigma_{\phi\phi} = \Delta P/2$, which are the expressions valid for an overpressured spherical cavity in an infinite elastic medium (Timoshenko and Goodier, 1982). Figure 1b shows tangential stress at $r = R_i$ plotted against R_o/R_i, and clearly the above limit is rapidly approached. For example, the stresses differ only by about 10% from $\Delta P/2$ for a value of $R_o/R_i = 3$. A search of the literature gives the impression that inclusions are commonly smaller than this with respect to their hosts. However, this is a matter that may merit more documentation. In the following calculations, we assume R_o/R_i to be large. The fact that this limit is rapidly attained suggests that the results are unlikely to differ substantially from those of a calculation allowing for a more realistic crystal shape or nonconcentric position of the inclusion. A more important factor is the inclusion shape. For example, the tangential stress at the wall of a cylindrical inclusion—a shape quite often observed (Roedder, 1965; Leroy, 1979)—would be equal to ΔP, i.e., twice as large as for a spherical inclusion. Inclusions with corners or irregularities are likely to produce stress concentration effects rendering them still less stable. The spherical case corresponds to conditions most favorable for the crystal to be able to withstand a given overpressure.

Decompression of the contents of a melt inclusion

We now give equations describing the contents of an inclusion subjected to a change in pressure, assuming that silicate melt and a pure gas phase are in thermodynamic equilibrium and that no crystallization takes place during ascent of the magma. The amounts of exsolved gas and dissolved volatiles and the density of the inclusion contents are functions of the internal pressure, the initial conditions, and the difference between the internal and external pressures, as this last controls the volume of the inclusion.

Mass conservation for the whole inclusion and of the volatile species read

$$m_l + m_g = \text{M} (= m_{lo} + m_{go}) \tag{8}$$
$$m_g + m_d = m_{go} + m_{do} \tag{9}$$

where subscripts l, g, and d refer to liquid, exsolved gas, and dissolved volatiles, respectively. M is the total mass of the contents of the inclusion, and the subscript o refers to the initial pressure $P_{\text{int}} = P_o$. If x is the mass fraction of the liquid made up of volatile molecules, then

$$m_d = x\cdot m_l. \tag{10}$$

Rearranging these gives the following equation for the mass fraction of gas (λ_g) at some new pressure $P_{\text{int}} = P$:

$$\lambda_g = \frac{m_g}{\text{M}} = \frac{\lambda_{go}(1 - x_o) + x_o - x}{(1 - x)}. \tag{11}$$

The volume equations are

$$V = V_l + V_g = V_o + \Delta V \tag{12}$$

$$V_l = \frac{m_l}{\rho_l} = \frac{m_{lo} - (m_g - m_{go})}{\rho_l} \tag{13}$$

$$V_g = \frac{m_g}{\rho_g} \tag{14}$$

in which the densities of gas (ρ_g) and liquid (ρ_l) will be given as equations of state. Substituting from Equations 12 and 13 into 14 we obtain

$$\lambda_g\left(\frac{1}{\rho_g} - \frac{1}{\rho_l}\right) = \lambda_{go}\left(\frac{1}{\rho_{go}} - \frac{1}{\rho_l}\right) + \lambda_{lo}\left(\frac{1}{\rho_{lo}} - \frac{1}{\rho_l}\right) + \frac{\Delta V}{\rho_o V_o} \tag{15}$$

where ρ_o is the initial bulk density of the inclusion contents. Combining Equation 15 with 11 and 6 gives

$$\left(\frac{1}{\rho_g} - \frac{1}{\rho_l}\right)\left[\frac{\lambda_{go}(1 - x_o) + x_o - x}{(1 - x)}\right] = \lambda_{go}\left(\frac{1}{\rho_{go}} - \frac{1}{\rho_l}\right) + \lambda_{lo}\left(\frac{1}{\rho_{lo}} - \frac{1}{\rho_l}\right) + \frac{\Gamma\Delta P}{\rho_o} \tag{16}$$

which upon substitution for ρ_g, ρ_l, and x is an equation between P_{int} (the internal pressure) and ΔP. The density of the liquid at pressure P is

$$\rho_l = \rho_{la}\left(1 + \frac{P - P_a}{\beta_l}\right) \tag{17}$$

where ρ_{la} is the density at atmospheric pressure P_a and β_l is the bulk modulus of silicate melt. For the gas phase, we assume

$$\rho_g = \frac{P}{\text{A}T} \tag{18}$$

where T is the temperature and A the ratio of the molar gas constant and the molecular weight of the gas species.

Because the rise of the magma during an eruption can be very rapid, we might suppose it necessary to use an adiabatic law to compute ρ_g at P. Because generally small mass fractions of gas are present, however, the heat capacity of the gas is small compared with that of silicate melt and crystal, which should certainly behave almost isothermally. Furthermore, we will show that decompressions experienced by inclusions are small, and hence we consider the system to be isothermal. To calculate the mass fraction of dissolved volatile species, we use the simple form

$$x = s \cdot P^n \tag{19}$$

where s is the solubility coefficient and n is a dimensionless exponent whose value depends on the gas species involved (see Table 1).

The main aspects of the physical behavior are illustrated by considering three limiting cases. First, the contribution to pressure of the expansion of the liquid is assessed by neglecting the presence of a volatile species. Second, we consider an inclusion just at the saturation point at the initial pressure but in which no gas bubble is trapped. Third, we treat the case of a pure gas inclusion. Inclusions in which a mixture of silicate melt and gas is initially trapped will show behavior in between that of the latter two cases. Table 1 gives the numerical values of the constants used.

For a pure liquid inclusion, Equation 16 reduces to

$$(\rho_{lo}/\rho_l) - 1 = \Gamma \cdot \Delta P. \tag{20}$$

Overpressure inside the inclusion results because the bulk modulus of the melt is less than the elastic constants of the solid. Figure 2a shows P_{int} and ΔP calculated as a function of decreasing P_{ext} for inclusions of basaltic magma in olivine crystals. Results for inclusions of rhyolitic melt in quartz crystals do not differ greatly because the elastic constants involved are similar (Table 1). The intercepts at 0.1 MPa give P_{int} and ΔP relevant to a sample ejected during a subaerial eruption, and those at P_{ext} = 30 and 50 MPa correspond to conditions of submarine basalts erupted at H_2O depths of 3 and 5 km. These results illustrate the simple fact that the crystal cannot expand sufficiently to accommodate the liquid. The inclusion is unable to decompress appreciably, and on arrival at the surface the interior pressure is typically between 80% and 90% of the initial pressure.

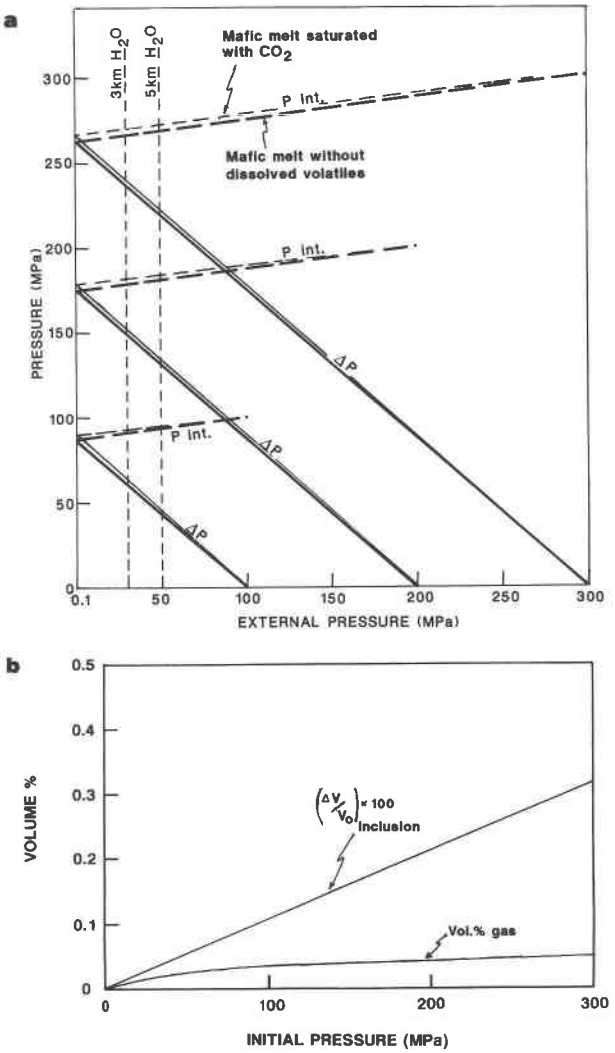

Fig. 2. (a) Calculations of P_{int} (dashed curves) and ΔP (solid curves) as a function of external pressure for inclusions of mafic melt. The heavy curves are for melt without dissolved volatiles, and the lighter curves are for mafic melt just saturated with pure CO_2 at P_o. Initial pressures are 100, 200, and 300 MPa. The intercepts at 0.1, 30, and 50 MPa give values of these variables at the Earth's surface during subaerial and submarine eruptions. (b) Fractional deformation of the inclusion and vol% gas within the inclusion for P_{ext} = 1 atm plotted as a function of the initial pressure.

TABLE 1. Physical constants used in calculations

Solubility for CO_2 in mafic melt (see Eq. 20)	$x = 4.4 \times 10^{-12} P^{1.0}$	Stolper and Holloway (1988)
for H_2O in mafic melt	$x = 6.8 \times 10^{-6} P^{0.7}$	Hamilton et al. (1964)
for H_2O in felsic melt	$x = 4.11 \times 10^{-6} P^{0.5}$	Burnham and Jahns (1962)
Density of mafic melt at P = 1 atm	2700 kg m^{-3}	
Density of felsic melt at P = 1 atm	2300 kg m^{-3}	
Young's modulus of olivine at 1200 °C	1.97×10^{11} Pa	Gebrande (1982)
Poisson's ratio	0.246	Gebrande (1982)
Young's modulus of quartz at 900 °C	9.0×10^{10} Pa	Gebrande (1982)
Poisson's ratio	0.2	Gebrande (1982)
Bulk modulus of mafic melt	1.2×10^{10} Pa	Murase and McBirney (1973)
of felsic melt	2.0×10^{10} Pa	Murase and McBirney (1973)

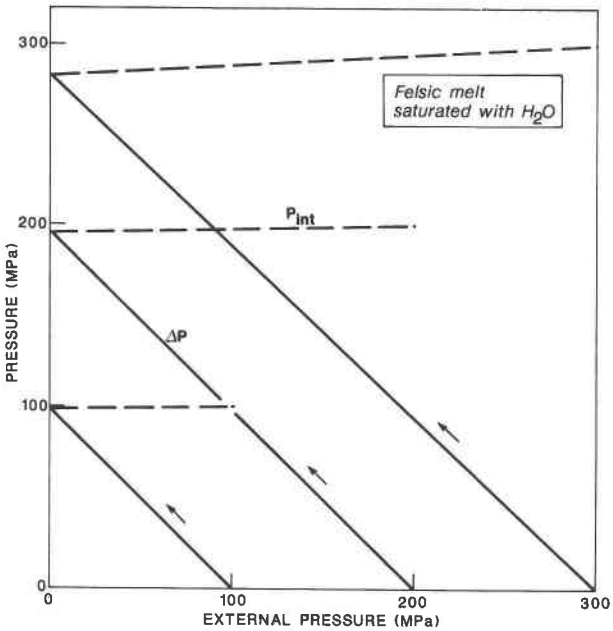

Fig. 3. Calculations of P_{int} and ΔP as a function of external pressure for an inclusion of felsic melt just saturated at the initial pressure with H_2O within a quartz crystal.

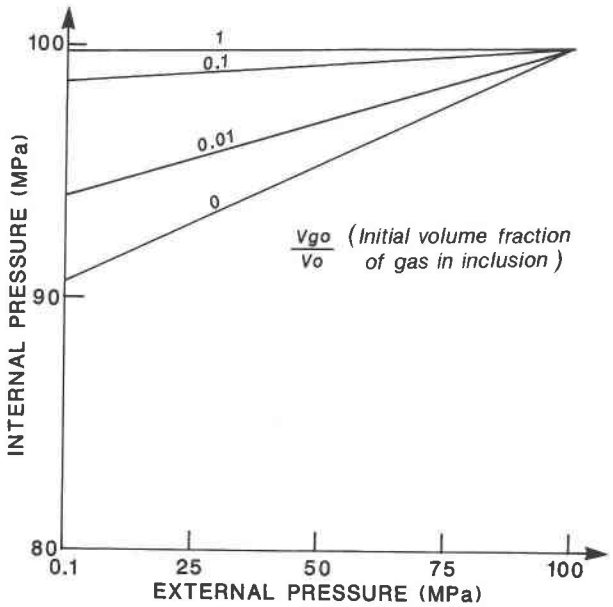

Fig. 4. Calculations of ΔP as a function of external pressure for inclusions within olivine crystals containing mafic melt and different amounts of pure CO_2 gas at the initial pressure. Note the expanded vertical scale compared with the graphs of Figures 2 and 3. The presence of a gas bubble leads to higher overpressures within the inclusion for a given external pressure.

For a melt just saturated at the initial pressure P_o with respect to a pure gas phase, i.e., $x_o = sP_o^n$ and $\lambda_{go} = 0$, Equation 16 reduces to

$$\left(\frac{1}{\rho_g} - \frac{1}{\rho_l}\right)\left(\frac{x_o - x}{1 - x}\right) = \left(\frac{1}{\rho_{lo}} - \frac{1}{\rho_l}\right) + \frac{\Gamma \cdot \Delta P}{\rho_{lo}}. \quad (21)$$

Calculations using Equation 21 for the case of a basaltic liquid saturated with pure CO_2 give results for ΔP very slightly higher than the case of a pure liquid inclusion for a given external pressure (Fig. 2a). The difference is small because expansion of the liquid keeps the pressure high within the inclusion and most volatile molecules remain in solution. Figure 2b shows, for the same calculations, the volume percentage of gas present in the inclusion and the volumetric deformation $(\Delta V/V_o) \times 100\%$ when $P_{ext} = 0.1$ MPa. Indeed very little gas exsolves. For the same reason, the behavior is insensitive to the form of the solubility law and hence the chemical composition of the volatile species. Quantitative results for mafic melt just saturated with a pure H_2O gas phase are similar. Figure 3 shows results for an inclusion within a quartz crystal containing rhyolitic melt just saturated with a pure H_2O gas phase at the initial pressure P_o. The ΔP is a little higher than for mafic systems, owing to the somewhat greater rigidity of quartz.

Figure 4 shows the case of an inclusion containing a CO_2 gas bubble as well as basaltic melt at the time of trapping (i.e., $\lambda_{go} \neq 0$). All calculations are for an initial pressure of 100 MPa. The curves are for different initial volume fractions of gas (V_{go}/V_o). The lowermost curve corresponds to $V_{go}/V_o = 0$ and the uppermost curve to a pure vapor inclusion in which the limit (Eq. 16) simplifies to

$$\left(\frac{1}{\rho_g} - \frac{1}{\rho_{go}}\right) = \frac{\Gamma \cdot \Delta P}{\rho_{go}}. \quad (22)$$

The more gas present initially in the inclusion, the higher is ΔP for a given external pressure (Fig. 4). This is because of the greater expansion of gas compared with liquid for a given pressure change.

The main conclusion of this analysis is that inclusions are unable to decompress by appreciable amounts by elastic expansion of the host crystal. If substantial cooling were to accompany rise in the volcanic conduit, larger decompressions would be possible because of the somewhat greater coefficient of thermal expansion of the melt compared with that of the crystal. However, this seems unlikely to be important in the vast majority of cases. This conclusion is more or less independent of the chemical compositions of lava and volatile species. The preservation of melt inclusions thus depends principally on the capacity of host crystals to withstand the applied stresses. We now try to estimate the conditions under which the fracture of mineral grains should occur.

Fracturing of silicate minerals

The tensile strength of an idealized, perfectly homogeneous crystal might in principle be expected to be on the order of the interatomic bond strength. In practice,

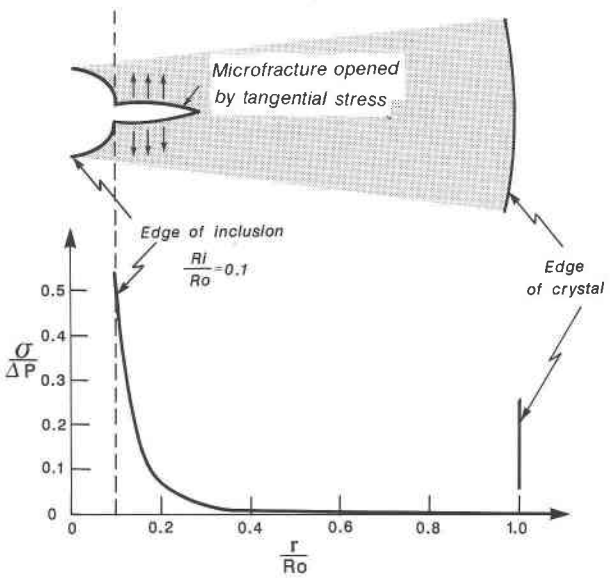

Fig. 5. Opening of a radially oriented crack in a host crystal. Normalized tangential stress is shown as a function of dimensionless radial coordinate within the crystal. The conclusion is that appreciable tangential stresses are only available to open a crack over a distance on the order of the inclusion radius.

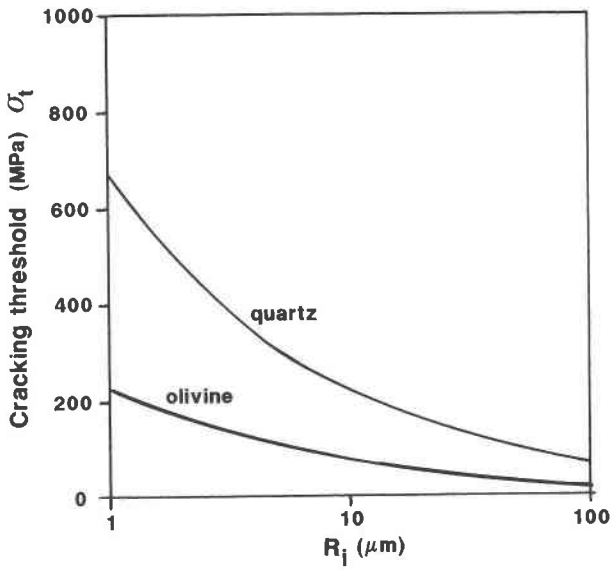

Fig. 6. The tensile stress at which olivine and quartz grains are expected to fail as a function of inclusion radius, calculated using Equation 23. Olivine is predicted to be weaker for a given inclusion size because of its apparently lower surface energy when compared with quartz.

however, microfractures are always likely to be present in the form of small growth defects, for example, and fracturing of the crystal essentially involves supplying the surface energy to force open such a preexisting microfracture. In a simple two-dimensional geometry, surface energy can be simply related to the normal tensile stress (σ_t) required to open a crack by the theory of Griffiths (e.g., Timoshenko and Goodier, 1982). This involves balancing the reduction in strain energy, associated with the tensile stresses, with the increase in surface energy, both of which result from opening the fissure. This energy balance leads to

$$\sigma_t = \sqrt{\frac{4E\nu}{\pi c}} \tag{23}$$

where E is Young's modulus, ν is the fracture surface energy, and c is the length of the preexisting microfracture on which the crack nucleates. The generalization to three dimensions is a difficult problem, only partially solved. The current situation is not strictly two dimensional; however, for small cracks this may be a reasonable approximation. Wanamaker et al. (1990) give a more elaborate reasoning based on a stress intensity factor at the irregularity on which the crack nucleates. Such factors are not well known however, and given these and other uncertainties, we prefer to follow the approach embodied by Equation 23, which should give at least the right order of magnitude for fracture strength (Jaeger and Cook, 1979, p. 101–105).

It is readily seen from Equation 23 that the smaller the microfracture, the more energy is required to nucleate a crack. For a given length c, σ_t can be interpreted as the tensile strength of the crystal. It is easily shown that, over a length scale comparable to the inclusion radius, the tangential stresses in the host crystal that open radial microcracks fall off by an order of magnitude (Fig. 5). Hence, in computing the fracture strength, it seems reasonable to assume that the length (c) of the microfissure on which a crack nucleates is of the same order as the inclusion radius.

Darot et al. (1985) used a microindentation technique to measure the fracture surface energy in single crystals of olivine and quartz as a function of temperature between 20 and 900 °C. Although the values for the upper part of this temperature range are appropriate for quartz crystals in rhyolitic melts, extrapolation is necessary in order to deduce a value for olivine in mafic magma. Their work suggests that appropriate values of ν are 0.1–0.2 J/m^2 for olivine and 3–4 J/m^2 for β quartz. These experiments were carried out in an inert Ar atmosphere. The presence of noninert species such as silicate melt or a CO_2/H_2O bubble tends to reduce fracture surface energy (Parks, 1984), and hence the above values should probably be considered as maxima.

Medium to large inclusions in igneous phenocrysts typically have radii in the range 20–100 μm. However, a survey of the literature indicates that inclusions considerably smaller than the above often occur. For example, Roedder (1965) described gaseous and liquid CO_2 inclusions on the order of 1 to a few μm. Using this range of length scale in Equation 23 and the values of Young's modulus given in Table 1, we obtain the range of tensile strengths shown in Figure 6: from approximately 20 to

200 MPa for olivine and 70 to 700 MPa for quartz. For spherical inclusions in infinite elastic media fracture occurs when $\Delta P = 2\sigma_t$. Thus, crystals may crack when ΔP exceeds approximately twice the above values.

The above estimates for the tensile strength of quartz are in remarkably good agreement with the values given by Roedder (1984, p. 71) and Bodnar et al. (1989) based on decrepitation experiments with igneous quartz samples. There is, however, an apparent discrepancy between the estimates of tensile strength of olivines based on our calculations and those proposed by Roedder (1984, p. 71) based on observations from natural samples. He suggests that the tensile strength of olivine is greater than that of quartz for a given inclusion size, which apparently contradicts the evidence of the measurements of fracture surface energy of Darot et al. (1985). The results of Wanamaker et al. (1990) and comparison with experimental data also seem to be in broad agreement with the current analysis in that olivine appears to be less resistant than quartz. The explanation may be that under natural conditions the decrepitation of inclusions can be delayed for a sufficient period by additional factors such that the inclusion is prematurely quenched or may be related to crack-healing phenomena (Wanamaker et al., 1990). This seems to be an aspect worthy of attention and of considerable importance for deductions made from natural inclusion-bearing olivines.

The above qualitative arguments seem in good accord with the observed size dependence of decrepitation pressures. Although the tensile strengths of igneous crystals under natural conditions are not known accurately, reasonably reliable maximum values can be estimated, and the overpressures we calculate commonly exceed these strengths. Fracture of host crystals is indeed commonly observed (e.g., Roedder, 1965; Harris and Anderson, 1983; Anderson et al., 1989), and in some examples, unfractured inclusions may be the exception rather than the rule. Since unfractured inclusions are generally selected for study, it is appropriate to consider whether this implies a strong sample bias.

The volatile contents of inclusions

Numerous techniques have been used to measure the volatile contents of melt and gas inclusions. Discrepancies between results are due partly to analytical difficulties and partly to differences between techniques. For example, infrared techniques measure only volatiles dissolved within a small volume of the glass (e.g., Fine and Stolper, 1986), whereas the vacuum fusion technique measures the entire contents of inclusions (Harris, 1981), thus integrating any gradients and incorporating exsolved gas into the analysis. We do not attempt a full discussion of these many data here but discuss some examples in the light of the foregoing calculations to show how our analysis may be used to provide a framework for interpreting such observations.

Until cracking occurs, the internal pressure remains high and most volatile molecules remain in solution. It is readily deduced from Equation 17, however, that only a small fractional volume change is sufficient to allow the liquid to expand and relieve the overpressure inside the inclusion. Consider, for example, a phenocryst ejected during a subaerial eruption with 100 MPa overpressure inside an inclusion. The fractional volume change required to allow the liquid inside to decompress to atmospheric pressure is

$$\frac{\rho_l(100\text{ MPa}) - \rho_l(0.1\text{ MPa})}{\rho_l(0.1\text{ MPa})} = \frac{\Delta P}{\beta_l} = \frac{(100 - 0.1) \times 10^6}{1.2 \times 10^{10}} \sim 10^{-2}$$

i.e., a volume change of approximately 1%. Such a small volume change might easily be accommodated by a set of small cracks in the inclusion walls. Cracking thus causes the melt to become strongly supersaturated with respect to volatiles. Bubble nucleation and growth should ensue, and given enough time, cracks can propagate to the edge of the crystal and degassing of the melt can proceed. This process may, however, be interrupted because on eruption the sample is rapidly cooled and the melt can be quenched to glass, thus trapping the volatiles in solution.

Results from silicic inclusions within quartz crystals (Table 2) show that the amounts of H_2O dissolved in the glass are generally less than that corresponding to a saturation pressure of approximately 200 MPa. Such values agree quite well with the fracture limit of quartz crystals estimated for reasonably large inclusions such as those commonly analyzed. For example, observations on Bishop Tuff inclusions of Anderson et al. (1989) indicate that many host crystals are cracked. Inclusions analyzed in this study were relatively large (on the order of 10–100 μm diameter). Not all inclusions are cracked however. Those intact have bubbles occupying approximately 0.2–0.4 vol% of the inclusion, which is consistent with the values calculated. Cracked inclusions have higher volume fractions of gas and less volatiles dissolved in the remaining glass. The above saturation pressures give a minimum pressure for the formation of the crystals and their inclusions. Were the pressure of formation to have been significantly higher, however, it seems likely that all such large inclusions would have cracked as a result of dilatation of the melt. The observation that some are still intact suggests that the inclusions were indeed formed at approximately 200 MPa under or close to gas saturation conditions, as suggested by Anderson et al. (1989).

The first systematic description of the appearance of melt and gas inclusions in mafic ejecta is that of Roedder (1965). He distinguished inclusions composed almost entirely of glass with small bubbles similar in size to that predicted by the results shown in Figure 2b from those containing liquid or gaseous CO_2, or both, and occupying a much larger volume fraction of the inclusion. In some

TABLE 2. Measured volatile contents of melt inclusions

Magma type, locality	Host crystal (condition)	Deposit	Measured volatiles (wt%)	Sat. *P* (MPa)
Rhyolite, Bishop Tuff, subaerial	quartz (many fractured, anals. on unfrac.)	Plinian	5.7 (H_2O) (max: 6.8)	190 (270)
		Ash flow	3.8 (H_2O) (max: 4.3)	85 (110)
Rhyolite, Bandelier Tuff, subaerial	quartz (not stated)	L. Plinian	4.0 (H_2O) (max: 7.3)	95 (310)
		L. ash flows	1.7 (H_2O) (max: 3.0)	17 (53)
		U. Plinian	2.1 (H_2O) (max: 2.6)	26 (40)
		U. ash flows	0.8 (H_2O) (max: 1.9)	4 (21)
Rhyolite, Taupo Volcanic Zone, subaerial	pyroxene, plagioclase, magnetite, quartz (not stated)	Taupo Plinian	4.3 (H_2O) (max: 4.5)	110 (120)
		Hatepe Plinian	4.3 (H_2O) (max: 4.9)	110 (140)
		Okaia tephra	5.9 (H_2O) (max: 6.1)	210 (220)
Basalt, Kilauea, submarine (3 km H_2O depth)	olivine (fractured)	lava	0.31 (CO_2)	700
		flow	0.46 (H_2O)	8.0
Basalt, Kilauea, subaerial	olivine (fractured)	lava	0.08 (CO_2)	180
		flow	0.27 (H_2O)	3.7

Note: Data from Dunbar et al. (1989); Anderson et al. (1989); Sommer and Schramm (1983); Harris and Anderson (1983).

cases, this may be due to the opening of fractures and subsequent exsolution of gas, but it may often be because bubbles were present at the moment of trapping. The calculations shown in Figure 4 illustrate that, all else being equal, the overpressures developed within inclusions containing some initial fraction of gas are somewhat greater than for those with no initial gas. Roedder observed that cracking of olivine host crystals containing inclusions of mafic melt and liquid CO_2 is common. He describes trains of inclusions lying along healed or partly healed fractures in the host crystal, and many of the pictures of individual inclusions show the presence of small cracks. Roedder estimated densities of the CO_2-rich gas phase at the time of trapping to be 700–900 kg/m^3. For temperatures of 1200 °C these densities correspond to pressures 400–700 MPa (Bottinga and Richet, 1981). These values correspond approximately to the upper range of, though are generally somewhat greater than, our estimates of fracture threshold obtained for inclusions of the size described by Roedder (1965) (1 to a few μm diameter). In short, agreement with the quantitative analysis presented here is not as good as for quartz, but it is not too bad given the uncertainties in fracture surface energies and the limitations of our two-dimensional consideration of crack initiation.

The data of Harris and Anderson (1983) provide an interesting comparison between mafic samples erupted under subaerial conditions and under approximately 3 km of H_2O (Table 2). The calculations presented in the current paper provide a framework to interpret these observations. Neglecting the presence of H_2O, the concentrations of CO_2 given correspond to saturation pressures of approximately 200 MPa for the subaerial sample and 700 MPa for the submarine sample. Both of these pressures are higher than the estimated tensile strength of olivine for these fairly large ($\approx$100 μm) inclusions, and indeed both inclusions show broad cracks traversing the host olivines (Figs. 1–3 of Harris and Anderson, 1983). The vacuum fusion technique used gives values higher than those obtained by IR spectroscopy (Fine and Stolper, 1986), and so the above saturation pressures may be somewhat overestimated. However, the precise values do not matter to a broad interpretation of these data. Seismic studies of Kilauea (Ryan, 1988) indicate the presence of large reservoirs of magma beneath the volcano at depths of 2–6 km (approximately 50–150 MPa). The phenocrysts in the subaerially erupted sample may plausibly be interpreted to have formed in the shallow storage zone of Kilauea. This would also imply that this storage zone is saturated with a gas phase, as has been suggested on the basis of gas emission measurements (Gerlach and Graeber, 1985) and the physical regimes of Kilauean eruptions (Vergniolle and Jaupart, 1990).

Our calculations indicate that if the sample from the submarine eruption were to have originated at 700 MPa, it is unlikely to have resided for any significant time in the shallow storage zone. If it had, the host crystals would have experienced an overpressure approximately equal to 600 MPa. They would have decrepitated therefore and exsolved gas from the melt until equilibrium with the ambient pressure of approximately 100 MPa was attained. Recent work on the nucleation and growth of CO_2 bubbles in basaltic melt (Bottinga and Javoy, 1990) suggests that because of the high surface energy of such bubbles quite large supersaturations may be required for exsolution to occur. Thus it seems plausible that this sample may have been preserved by the sluggish kinetics of exsolution of CO_2 transferred rapidly from 700 MPa

to the eruption site of 30 MPa and quenched by interaction with the sea water before the gas could exsolve.

An interesting implication of sluggish exsolution kinetics concerns eruptions in which transitions occur from Plinian to Peléen regimes and eventually to lava effusion. In such cases, the transit time of magma from the storage reservoir to the surface may increase from tens of minutes to weeks. Thus, it seems plausible that in the explosive regime short transit times and rapid quenching by violent mixing with the atmosphere could combine to preserve unstable inclusions before complete decrepitation occurs. At the other extreme, sluggish lava effusion and slow cooling at close to atmospheric pressure are likely to give sufficient time for exsolution. A feature of the data from the Bandelier Tuff is that volatile contents measured on inclusions in each of the Plinian phases are greater than those in the associated ash flow units. Unfortunately, Sommer and Schramm (1983) do not mention whether cracked inclusions are more common in the ash flow deposits than in the Plinian deposits. This has been observed, however, in plagioclase phenocrysts of the rhyodacytic deposits associated with the Crater Lake caldera (Bacon et al., 1988). Intact melt inclusions with high volatile contents are common in the Plinian deposit, but in the ash flow deposits the melt inclusions have all decrepitated.

A possible explanation is that the transfer time from the magma chamber to the surface for the ash flow deposits was sufficiently high that once inclusions had cracked, gas bubbles had time to nucleate and expand and decrepitate the inclusions. In the Plinian phase, however, the magma rose so rapidly to the surface that the inclusions were quenched before decrepitation could occur. The chamber seems certain to be at its maximum pressure during the Plinian phase, and although the total mass flux may be higher during ash flow eruption because of enlargement of the conduit system, the eruption velocity is likely to be greatest (and hence the transfer time the shortest) during the Plinian phase. Current knowledge of the exsolution kinetics of volatiles from silicate melts is insufficient to make a firm quantitative statement, but it seems possible that systematic differences in the volatile contents measured in inclusions may be due to changes in the physical regime of eruption, even if the magma composition were the same.

Conclusions

Our analysis shows that for virtually all common inclusion sizes the host crystal acts as an infinite elastic medium. The large elastic moduli of silicate minerals prevent inclusions from decompressing, and upon eruption, the grains experience dilatational stresses on the order of the pressure of formation of the inclusion. Small bubbles may form, but most volatile molecules remain in solution until the crystal cracks. The fracture threshold of host crystals is predicted to decrease with increasing inclusion size because the stresses required to open a crack are only available over a narrow zone adjacent to the edge of the inclusion. A major implication of this is that the deeper the origin of an erupted magma, the more likely inclusions are to decrepitate. In such cases, however, very small inclusions may nevertheless be preserved and could provide valuable information on the state of the magma prior to eruption if difficulties of measurement can be overcome. A second important point is that in some cases sluggish kinetics may delay exsolution sufficiently for quenching to preserve inclusions before complete decrepitation can occur. In such cases the preservation of inclusions would critically depend on the time of transit from magma chamber to surface and subsequent quenching relative to the time required for exsolution to occur. Thus preservation of inclusions may in some cases be linked to the physical regime of eruption.

Acknowledgments

I would like to thank Fred Anderson, Charlie Bacon, Claude Jaupart, Jean-Paul Poirier, and Christine Skirius for fruitful discussions and Fred Anderson for a challenging and thoughtful review of the manuscript.

References cited

Anderson, A., Newman, S., Williams, S., Druitt, T.H., Skirius, C., and Stolper, E. (1989) H_2O, CO_2, Cl and gas in Plinian and ash-flow Bishop rhyolite. Journal of Geology, 17, 221–225.

Bacon, C.R., Newman, S., and Stolper, E. (1988) Preeruptive volatile content, climactic eruption of Mount Mazama, Crater Lake, Oregon. Geological Society of America Abstracts with Programs, 20(7), A248.

Blake, S. (1984) Volatile oversaturation during the evolution of silicic magma chambers as an eruption trigger. Journal of Geophysical Research, 89, 8237–8244.

Bodnar, R.J., Binns, P.R., and Hall, D.L. (1989) Synthetic fluid inclusions—VI. Quantitative evaluation of the decrepitation behaviour of fluid inclusions in quartz at one atmosphere confining pressure. Journal of Metamorphic Geology, 7, 229–242.

Bottinga, Y., and Javoy, M. (1990) Mid-ocean ridge basalt degassing: Bubble nucleation. Journal of Geophysical Research, 95, 5125–5131.

Bottinga, Y., and Richet, P. (1981) High pressure and temperature equation of state and calculation of the thermodynamic properties of gaseous CO_2. American Journal of Science, 281, 615–660.

Burnham, C.W., and Jahns, R.H. (1962) A method for determining the solubility of water in silicate melts. American Journal of Science, 281, 615–660.

Darot, M., Guegen, Y., and Benchemam, G.R. (1985) Ductile-brittle transition investigated by micro-indentation: Results for quartz and olivine. Physics of Earth and Planetary Interiors, 40, 180–186.

Dunbar, N., Hervig, R.L., and Kyle, P.R. (1989) Determination of preeruptive H_2O, F and Cl contents of silicic magmas using melt inclusions: Examples from Taupo volcanic centre, New Zealand. Bulletin of Volcanology, 51, 177–184.

Fine, G., and Stolper, E. (1986) Dissolved carbon dioxide in basaltic glasses: Concentrations and speciation. Earth and Planetary Science Letters, 76, 263–278.

Gebrande, H. (1982) Elastic wave velocities and constant of elasticity of rock and rock-forming minerals. In G. Angenheister, Ed., Physical properties of rocks, Landalt-Bornstein series, group V, vol. 1b, 3.1.2, p. 8–34. Springer-Verlag, Berlin.

Gerlach, T.M., and Graeber, E. (1985) Volatile budget of Kilauea Volcano. Nature, 313, 273–277.

Gillet, P., Ingrin, J., and Chopin, C. (1984) Coesite in subducted continental crust: P-T history deduced from an elastic model. Earth and Planetary Science Letters, 70, 426–436.

Green, H.W., and Guegen, Y. (1983) Deformation of peridotite in the mantle and extraction by Kimberlite: A case history documented by fluid and solid precipitates in olivine. Tectonophysics, 92, 71–92.

Hamilton, D.L., Burnham, C.W., and Osborn, E.F. (1964) The solubility of water and effects of oxygen fugacity and water content on crystallisation in mafic magmas. Journal of Petrology, 5, 21–39.
Harris, D.M. (1981) The concentration of CO_2 in submarine tholeiitic basalts. Journal of Geology, 89, 689–701.
Harris, D.M., and Anderson, A.T. (1983) Concentrations sources and losses of H_2O, CO_2 and S in Kilauean basalt. Geochimica et Cosmochimica Acta, 47, 1139–1150.
Ho-Liu, P., Johnson, C., Montagner, J.-P., Kanamori, H., and Clayton, R.W. (1990) Three-dimensional attenuation structure of Kilauea East Rift Zone, Hawaii. Bulletin of Volcanology, in press.
Jaeger, J.C., and Cook, N.G.W. (1979) Fundamentals of rock mechanics, p. 593. Chapman and Hall, London.
Leroy, J. (1979) Contribution à l'étallonage de la pression interne des inclusions fluides lors de leur décrépitation. Bulletin de Minéralogie, 102, 584–593.
Murase, T., and McBirney, A.R. (1973) Properties of some common igneous rocks and their melts at high temperature. Bulletin of the Geological Society of America, 84, 3563–3593.
Parks, G.A. (1984) Surface and interfacial face energies of quartz. Journal of Geophysical Research, 89, 3997–4008.
Prud'homme, R.K., and Bird, R.B. (1978) The dilatational properties of suspensions of gas bubbles in incompressible Newtonian and non-Newtonian fluids. Journal of Non-Newtonian Fluid Mechanics, 3, 261–279.
Roedder, E. (1965) Liquid CO_2 inclusions in olivine-bearing nodules and phenocrysts from basalts. American Mineralogist, 50, 1746–1782.
——— (1984) Fluid inclusions. In Mineralogical Society of America Reviews in Mineralogy, 12, 644 p.
Ryan, M.P. (1988) The mechanics and internal structure of active magma systems: Kilauea volcano, Hawaii. Journal of Geophysical Research, 93, 4213–4248.
Sommer, M.A., and Schramm, L.S. (1983) An analysis of the water concentrations in silicate melt inclusions in quartz phenocrysts from the Bandelier Tuff, Jemez mountains, New Mexico. Bulletin of Volcanology, 46, 299–320.
Stolper, E., and Holloway, J.R. (1988) Experimental determination of the solubility of carbon dioxide in molten basalt at low pressure. Earth and Planetary Science Letters, 87, 397–408.
Tait, S.R., Jaupart, C., and Vergniolle, S. (1989) Pressure, gas content and eruption periodicity of a shallow, crystallising magma chamber. Earth and Planetary Science Letters, 92, 107–123.
Timoshenko, S.P., and Goodier, J.N. (1982) Theory of elasticity, p. 567. McGraw Hill, Singapore.
Vergniolle, S., and Jaupart, C. (1986) Separated two-phase flow and basaltic eruptions. Journal of Geophysical Research, 91, 12842–12860.
——— (1990) Dynamics of degassing at Kilauea Volcano, Hawaii. Journal of Geophysical Research, 95, 2793–2809.
Wanamaker, B.J., Wong, T.-F., and Evans, B. (1990) Decrepitation and crack healing of fluid inclusions in San Carlos olivine. Journal of Geophysical Research, 95, 15, 623–15641.
Wilson, L., and Head, J. (1981) Ascent and eruption of basaltic magma on the Earth and moon. Journal of Geophysical Research, 86, 2971–3001.

Manuscript received August 31, 1990
Manuscript accepted September 11, 1991

Appendix 1. Dilatation of an overpressured inclusion by viscous flow of the host crystal

Following the analysis of Prud'homme and Bird (1978), we estimate a time scale for the viscous dissipation of stresses within a crystal containing an overpressured inclusion by assuming that the crystal is an incompressible Newtonian fluid that flows radially to make room for swelling of the inclusion. Referring to the geometry shown in Figure 1, the continuity equation reads

$$\frac{\partial}{\partial r}(\rho r^2 v_r) = 0 \qquad R_i < r < R_o \tag{A1}$$

where v_r is the radial velocity and ρ the density. The ρ is constant, and thus integration gives

$$v_r = \frac{R_i^2}{r^2}\cdot \dot{R}_i. \tag{A2}$$

The r component of the momentum equation reads

$$-\frac{\partial P}{\partial r} + \mu \frac{\partial}{\partial r}\left[\frac{1}{r^2}\frac{\partial}{\partial r}(r^2 v_r)\right] = 0 \tag{A3}$$

where P is the pressure. We may deduce from Equations A3 and A1 that $\partial P/\partial r = 0$, i.e., that pressure is spatially uniform in the crystal at any given moment. Equating the radial stress within and just outside the inclusion at $r = R_i$ gives

$$P_{\text{int}} + (\tau_{rr})_{r=R_{i-}} = P + (\tau_{rr})_{r=R_{i+}} + 2\frac{\sigma}{R_1} \tag{A4}$$

where τ_{rr} is the radial component of the stress tensor, P_{int} is the pressure of the inclusion contents, and σ is the surface tension between the crystal and the inclusion contents. If we neglect surface tension and take the crystal to be very much more viscous than the contents of the inclusion, this simplifies to

$$P_{\text{int}} \approx P + (\tau_{rr})_{r=R_{i+}}. \tag{A5}$$

In addition, we have that

$$P_{\text{ext}} = P + (\tau_{rr})_{r=R_o}. \tag{A6}$$

From the velocity distribution, we obtain

$$\tau_{rr} = 4\mu \frac{R_i^2}{r^3}\dot{R}_i \tag{A7}$$

and hence

$$P_{\text{int}} - P_{\text{ext}} = 4\mu\left(\frac{1}{R_i} - \frac{R_i^2}{R_o^3}\right)\dot{R}_i \approx 4\mu\frac{\dot{R}_i}{R_i}. \tag{A8}$$

A characteristic time scale for the deformation is thus

$$R_i/\dot{R}_i \approx \frac{4\mu}{\Delta P}. \tag{A9}$$

Taking the example of an olivine crystal at the liquidus temperature of mafic magma ($\mu \approx 10^{21}$ Pa·s) and assuming ΔP to be on the order of 100 MPa, we obtain a time scale of approximately a million years. This implies that viscous release of elastic stresses may safely be neglected on the time scale of a volcanic eruption. During uplift of metamorphic rocks, temperatures are lower than the above and hence the appropriate viscosity is likely to be several orders of magnitude higher, correspondingly increasing the time scale of viscous flow. Thus, although tectonic uplift may take place over tens of millions of years, it seems unlikely that viscous deformation of crystals could play an important role in allowing an overpressured inclusion to decompress.